Geomechanics and Engineering, *Vol. 5, No. 6 (2013) 519-540*
DOI: http://dx.doi.org/10.12989/gae.2013.5.6.519

Optimum pile arrangement in piled raft foundation by using simplified settlement analysis and adaptive step-length algorithm

Keiji Nakanishi[1] and Izuru Takewaki[*2]

[1] *Institute of Technology, Shimizu Corporation, Koto-ku, Tokyo 135-8530, Japan*
[2] *Department of Architecture and Architectural Engineering, Kyoto University, Kyotodaigaku-Katsura, Nishikyo-ku, Kyoto 615-8540, Japan*

(Received January 17, 2013, Revised May 22, 2013, Accepted June 04, 2013)

Abstract. This paper presents an optimal design method for determining pile lengths of piled raft foundations. The foundation settlement is evaluated by taking into account the raft-pile-soil interaction. The analysis of settlement is simplified by using Steinbrenner's equation. Then the total pile length is minimized under the settlement constraint. An extended sequential linear programming technique combined with an adaptive step-length algorithm of pile lengths is used to solve the optimal design problem. The accuracy of the simplified settlement analysis method and the validity of the obtained optimal solution are investigated through the comparison with the actual measurement result in existing piled raft foundations.

Keywords: piled raft foundation; vertical load; optimum design; pile arrangement; settlement analysis; observed data; large-step numerical sensitivity

1. Introduction

Piled raft foundations, which are combinations of mat-slab foundations (raft) and friction piles, are often used recently as rational foundation systems enabling the smart settlement control and cost reduction (Randolph 1983, 1994, Ta and Small 1996, Poulos *et al*. 1997, Poulos 2001, Chow *et al*. 2001, Cunha *et al*. 2001, Prakoso and Kulhawy 2001, AIJ 2001a, Small and Zhang 2002, Liew *et al*. 2002, Reul and Randolph 2003, 2004, Fattah *et al*. 2013). These piled raft foundations are used both for low-rise and high-rise buildings.

There are some researches on the optimization of piled raft foundations. For example, Horikoshi and Randolph (1998), Valliappan *et al*. (1999), Kim *et al*. (2001), Kim *et al*. (2002), Reul and Randolph (2004), Leung (2010), Leung *et al*. (2010) have investigated the optimization of piled raft foundations for various design variables. Especially Reul and Randolph (2004) derived useful results based on data-based charts and Leung (2010) and Leung *et al*. (2010) formulated a comprehensive optimization problem and derived several significant and useful results by using a data-based pattern function for optimization. Furthermore Kim *et al*. (2002) introduced a genetic algorithm to optimize the piled-raft foundation assuming linear elastic pile-soil interaction. Although piled raft foundations are not treated, Chan *et al*. (2009) developed

∗Corresponding author, Professor, E-mail: takewaki@archi.kyoto-u.ac.jp

 ISSN: 2005-307X (Print), 2092-6219 (Online)

an automated optimal design method using a hybrid genetic algorithm for pile group foundation design. The design process includes a sizing and topology optimization for pile foundations. A local search operator by a fully stressed design approach is incorporated to tackle two shortcomings of a genetic algorithm, i.e., (i) large computation effort in searching the optimum design; and (ii) poor local search capability. Because nonlinear characteristics of soils need to be included in the interaction analysis for settlement among rafts, piles and soils in the piled raft foundations, the optimal design of piled raft foundations has difficulty. This brings structural and geotechnical engineers a number of repetitions of analysis for better design of piled raft foundations.

There are several settlement analysis methods for piled raft foundations. The first method is a three-dimensional finite element method which models all the foundations, piles and soils as finite elements. While this three-dimensional finite element method can simulate soil nonlinearities and interaction among rafts, piles and soils directly, it requires a great deal of computational time and memory and needs cumbersome tasks for the management of input and output data. The second method is a hybrid method combining a finite-element system for foundations and piles with soil springs under foundations and around piles evaluated by Steinbrenner's equation or Mindlin's equation. While this hybrid method has an advantage of a small number of finite elements, an assumption of a uniform half space for ground leads to lower accuracy for multi-layered grounds and an approximate repetition procedure is required in evaluating the nonlinear soil properties. Both methods have advantages and disadvantaged depending on aspects of evaluations. From the viewpoint of optimization of piled raft foundations, the hybrid method seems to be preferable.

A simplified settlement analysis method for piled raft foundations is proposed first in this paper. The method takes into account the raft-pile-soil interaction and uses Steinbrenner's equation. An optimal design problem is then formulated so as to determine pile lengths of piled raft foundations. The total pile length is aimed at being minimized under the settlement constraint on the foundation. A new extended sequential linear programming technique combined with an adaptive step-length algorithm of pile lengths is devised to solve the optimal design problem. It is shown that the pile grouping is effective for obtaining practically acceptable pile placements. The accuracy of the proposed simplified settlement analysis method and the validity of the obtained optimal solution are discussed through the comparison with the actual measurement results in existing piled raft foundations. The novelties of this paper are (1) to propose a simplified settlement analysis method for piled raft foundations, (2) to propose a new extended sequential linear programming technique combined with an adaptive step-length algorithm of pile lengths and (3) to verify the accuracy and reliability of the proposed methods through the comparison with the measured data.

2. Simplified settlement analysis

Consider a piled raft foundation as shown in Fig. 1. The foundation is subjected to an unsymmetric loading and soils around piles sustain additional shear stresses resulting from the friction around piles. Soils beneath the foundation and the piles also sustain vertical loads. Fig. 1 also shows the load-carrying mechanism of the piled raft foundation as explained above. The piled raft foundation is modeled here by a grid beam-spring model (hybrid model used in the FEM analysis (AIJ 2001a)) as shown in Fig. 2. The foundation beam is modeled by beam finite elements. The vertical resistance of a pile is modeled by a pile spring and the vertical resistance of soils beneath the foundation is represented by a soil spring. These resistances are explained in Sections

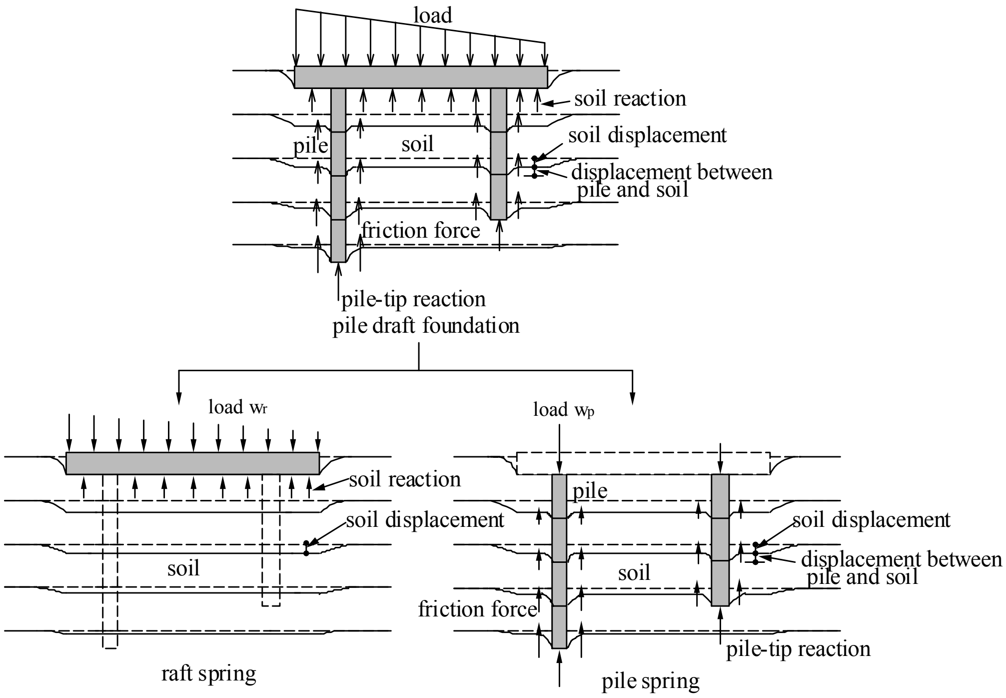

Fig. 1 Load-carrying mechanism of piled raft foundation

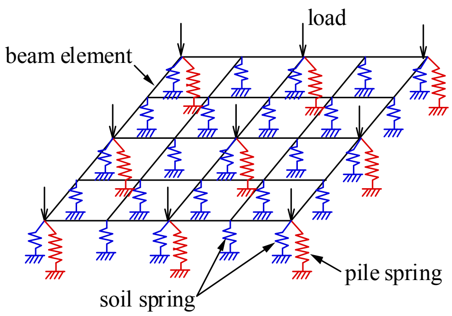

Fig. 2 Grid beam-spring model

2.2 and 2.3. Fig. 3 presents the friction-spring characteristic around a pile and Fig. 4 shows the pile-tip reaction-settlement relation. In Fig. 3, f_u: ultimate friction force, δ_u: ultimate displacement and K: stiffness before slippage. In addition, in Fig. 4, R_p: pile-tip load, A_p: pile cross-sectional area, S_p: settlement at pile tip, d_p: pile diameter, k_b: initial stiffness in the pile-tip load-settlement relation. It is well known that soils exhibit amplitude-dependent nonlinearities (Hardin and Drnevich 1972) and such nonlinearities are often modeled by an equivalent linear model. Fig. 5 indicates the soil stiffness reduction due to the increase of the vertical soil strain (Tamaoki *et al.* 1993a, b). The repetition for convergence is introduced in the evaluation of the Young's modulus of soil. Fig. 6 presents the flowchart of the settlement analysis.

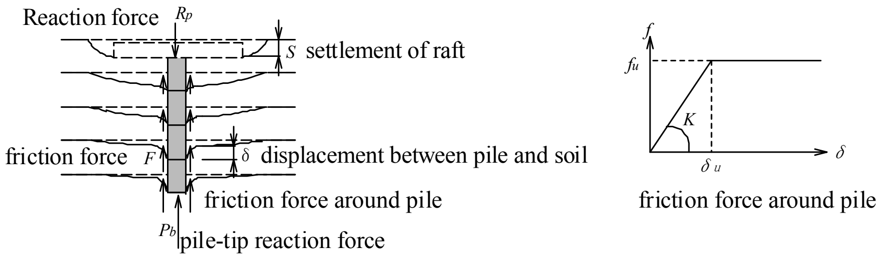

Fig. 3 Friction-spring characteristic of pile

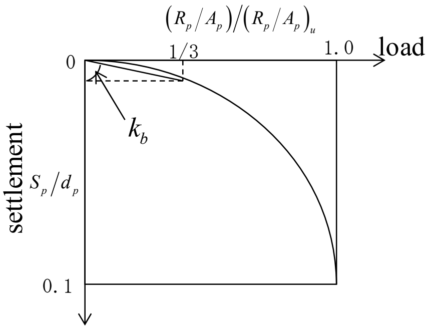

Fig. 4 Pile-tip load-settlement relation

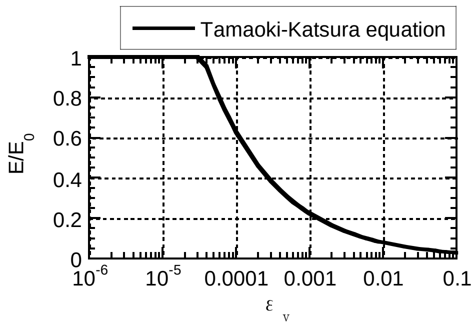

Fig. 5 Soil stiffness reduction for vertical soil strain

The foundation is described by beam models and the soil beneath the foundation and the pile supported by soils are modeled by Winkler-type springs based on the three-dimensional continuum theory of elasticity. More detailed explanation is shown below.

2.1 Initial Young's modulus and stiffness reduction for the vertical strain

The soil stiffness is obtained iteratively by using the following properties on the initial soil stiffness and stiffness reduction due to amplitude dependence.

$$E_0 = 2(1+\nu)\gamma V_S^2 / g \quad \text{for initial soil stiffness} \tag{1}$$

$$E/E_0 = 0.01\varepsilon_V^{-0.45} \quad \text{for stiffness reduction for the vertical strain } \varepsilon_V \tag{2}$$

where V_S is the shear wave velocity (m/s), ν is Poisson's ratio, g is the acceleration of gravity (m/s^2), γ is soil weight per unit volume (kN/m^3) and ε_V is the vertical strain evaluated by Steinbrenner's approximate solution. Eq. (1) presents the relation between Young's modulus and the shear modulus and Eq. (2) is from Tamaoki *et al.* (1993a, b).

2.2 Soil spring beneath foundation

The soil spring beneath the foundation is evaluated by computing the settlement of the raft using Steinbrenner's approximate solution (Steinbrenner 1934) for a semi-infinite half space extended to a multi-layered ground.

The vertical strain ε_V can be evaluated from the following settlement.

$$S_E = \left\{ \frac{I_S(H_1, v_{S1})}{E_{S1}} + \sum_{k=2}^{n} \frac{I_S(H_k, v_{Sk}) - I_S(H_{k-1}, v_{Sk})}{E_{Sk}} \right\} 4q \cdot \frac{B}{2} \tag{3}$$

where I_S (H_k, v_{Sk}) is the settlement coefficient for soil with thickness H_k and Poisson's ratio v_{Sk}, H_k (m) is the distance from the ground surface to the bottom of the k-th layer, E_{Sk} is the Young's modulus, B, L (m) are the foundation width and length, q (kN/m^2) is the distributed load. The expression of I_S (H_k, v_{Sk}) is shown in Appendix 1.

The soil spring K_{Ri} beneath the foundation concentrated to the joint of the foundation grid beams is evaluated by dividing the spring force P_i (kN) by the settlement S_i (m).

$$K_{Ri} = P_i / S_i \tag{4}$$

The settlement at the joint i can be obtained by

$$S_i = \sum_{j=1}^{n} S_{ij} \tag{5}$$

where S_{ij} is the settlement at the joint i subjected to the load at the joint j and is evaluated by Boussinesq's solution.

The interaction among the joints in the grid beams in the raft foundation is taken into account in the evaluation of the soil spring beneath the foundation.

2.3 Vertical spring defined at pile-top

The vertical spring K_{pi} (kN/m) defined at a pile-top is evaluated by dividing the pile into m elements of 1(m) and computing the friction forces F_j (kN) around the pile and the reaction force P_b (kN) beneath the pile-tip from the vertical displacements at the pile nodes in the settlement analysis in Section 2.2. The interaction between raft and pile is taken into account in calculating the pile friction force and the pile-tip reaction force under relative vertical displacements between the pile and soils beneath the foundation.

The vertical spring K_{pi} can be obtained by

$$K_{pi} = R_{pi} / S_i \tag{6}$$

where S_i (m) is the settlement at the pile-top in the settlement analysis in Section 2.2 and the total pile reaction R_{pi} (kN) is computed from

$$R_{pi} = \sum_{j=1}^{m} F_j + P_b \tag{7}$$

The relation of pile friction force and displacement is described by a bilinear model. The ultimate friction force f_u and the corresponding displacement δ_u are evaluated by the following equations.

$$f_u = \alpha N (\text{kN/m}^2), \quad \delta_u = 20\,\text{mm} \quad \text{for sand} \tag{8}$$

$$f_u = \beta q_u \,(\mathrm{kN/m^2}),\quad \delta_u = 10\,\mathrm{mm} \quad \text{for clay} \tag{9}$$

where α is 2.5 for buried pile and 3.3 for case-in-place reinforced concrete pile, β is 0.4 for buried pile and 0.5 for case-in-place reinforced concrete pile, N is the SPT count and q_u (kN/m^2) is the one-dimensional compressive strength. The limit displacements for sand and clay are based on experimental works. Eqs. (8) and (9) are from AIJ (2001b).

The pile-tip spring stiffness is computed from the secant stiffness at the design vertical load on the relation of pile-tip reaction R_p and pile-tip displacement S_p expressed by

$$\left(S_p/d_p\right)/0.1 = \gamma\left(R_p/R_{pu}\right) + \left(1-\gamma\right)\left(R_p/R_{pu}\right)^2 \tag{10}$$

where S_p (m) is the pile-tip settlement, d_p (m) is the pile diameter, γ is 0.2 for buried pile and 0.3 for case-in-place reinforced concrete pile, R_{pu} is the limit bearing strength (R_{pu} = 200N for buried pile in sand soil, R_{pu} = 3q_u for buried pile in clay soil, R_{pu} = 100N for case-in-place reinforced

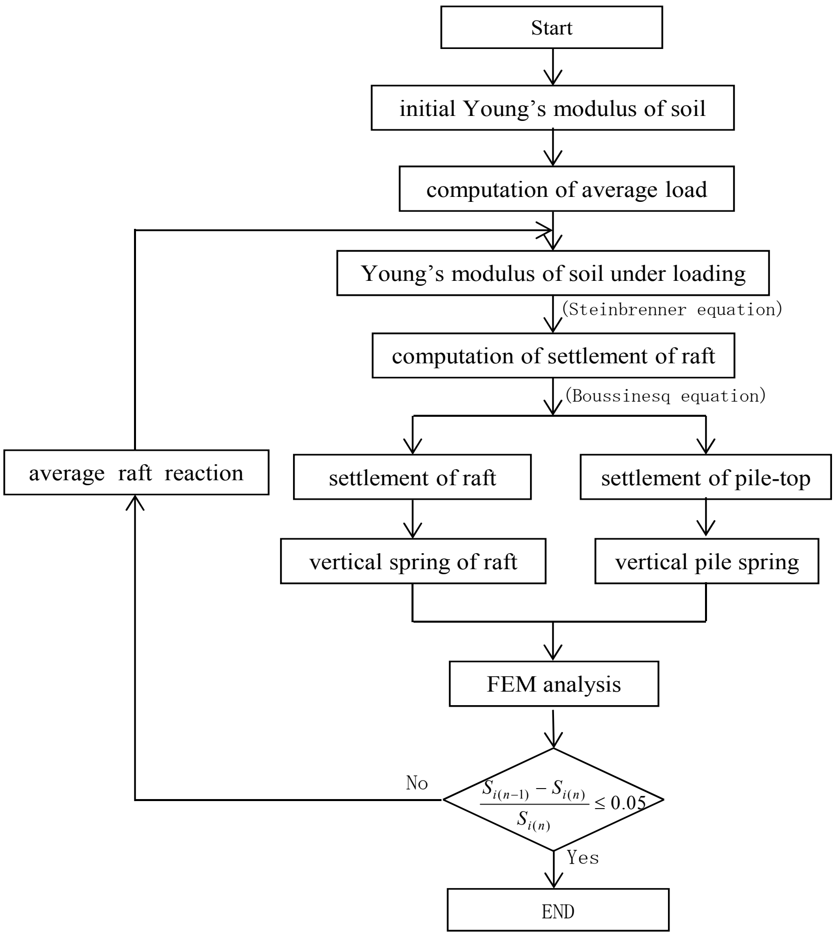

Fig. 6 Flowchart of settlement analysis (FEM analysis: Conducted using hybrid model in Fig. 2)

concrete pile in sand soil and R_{pu} =3 q_u for case-in-place reinforced concrete pile in clay soil). Eq. (10) is from AIJ (2001b).

Since the settlements at the pile-top and pile-tip and around piles computed in Section 2.2 are used in the present analysis, the interaction between the raft and the pile is taken into account in the evaluation of the vertical spring defined at pile-top.

It should be noted that the repetition for convergence is conducted in Sections 2.2 and 2.3 (see Fig. 6).

3. Optimal design method

3.1 Optimal design problem

It is commonly accepted in practice that serviceability is the principal criterion for the design of vertically loaded piled raft foundations of tall buildings. Furthermore, from the point of view of simplification and practicality, it is assumed here that the costs for the installation of the piled raft foundation are proportional to the total pile length.

Consider an optimal design problem so as to minimize the total pile length under the constraint on the settlement of a piled raft foundation under vertical loading. The pile diameters are specified and the lengths of the piles are the design variables. The optimal design problem is stated as follows:

$$\begin{aligned} &\text{Find} && \mathbf{L} = (L_1, L_2, \cdots, L_m) \\ &\text{so as to minimize} && W(L_1, L_2, \cdots, L_m) = \rho A \sum_{i=1}^{m} L_i \end{aligned} \tag{11}$$

$$\text{subject to} \quad S_i(L_1, L_2, \cdots, L_m) < S_a \quad (i = 1 \sim n) \tag{12}$$

In this problem, W: weight of piles, S_i: settlement of nodal point i, S_a: limit of settlement, L_j: length of pile j, m: number of piles, n: number of nodal points with settlement limit, ρ: pile density, A: pile cross-sectional area.

In the application of the sequential linear programming with variable step sizes, the first-order Taylor series expansion of the constraints is necessary. The constraint (11) on settlement can be expressed in terms of the first-order Taylor series expansion.

$$S_i(\mathbf{L}) = S_i(\mathbf{L}^0) + \sum_{j=1}^{m} \left(\frac{\partial S_i(\mathbf{L})}{\partial L_j} \Big|_{L=L^0} \times \Delta L_j \right) \le S_a \quad (i = 1 \sim n) \tag{13}$$

where $\mathbf{L}^0 = \{L_j^0\}$ denotes the set of pile lengths at the present design stage. The side constraints on pile lengths can be described as

$$L_j^L \le L_j^0 + \Delta L_j \le L_j^U \quad (j = 1 \sim m) \tag{14}$$

$$-\varepsilon_j \le \Delta L_j \le \varepsilon_j \quad (j = 1 \sim m) \tag{15}$$

Here L_j^L and L_j^U denote the lower and upper bounds on the length of pile i and ε_j is an admissible move limit of ΔL_j.

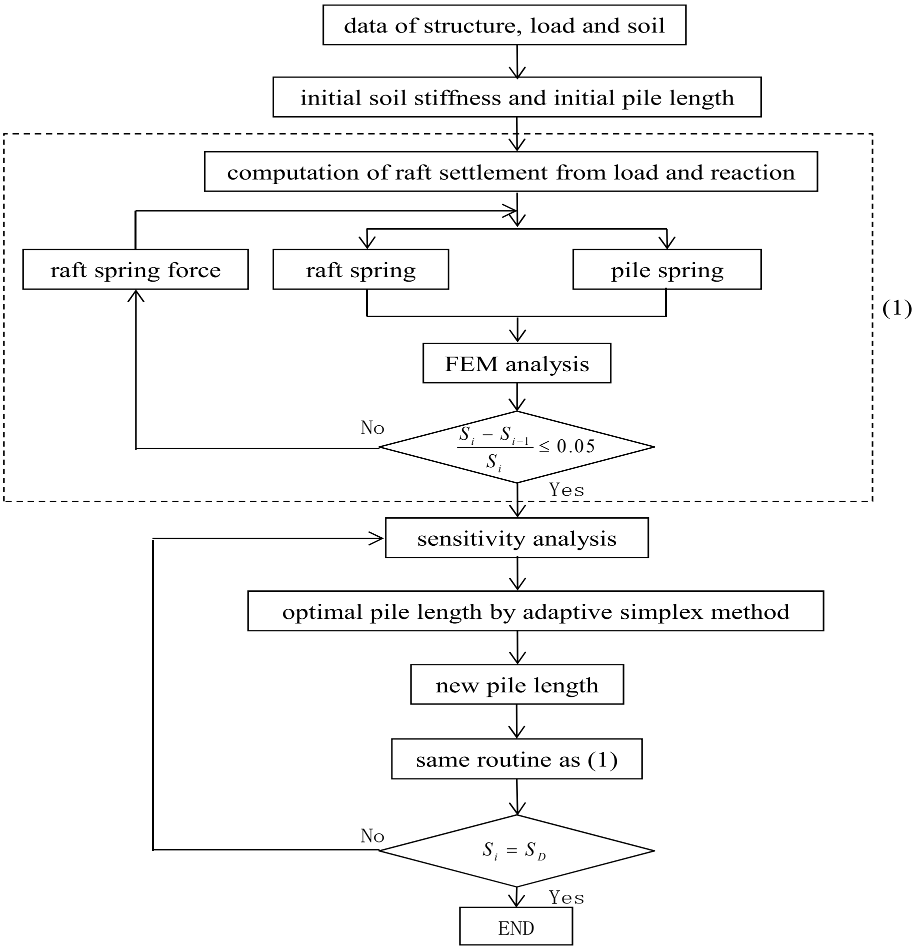

Fig. 7 Flowchart of optimization (FEM analysis: Conducted using hybrid model in Fig. 2)

3.2 Formulation of optimization procedure

Fig. 7 shows the flowchart of optimization. Each step may be explained as follows:

(1) Specify the initial set of sufficiently long pile lengths so that the constraint on foundation settlement is satisfied.

(2) Compute the raft spring stiffness and the pile spring stiffness from soil stiffness and soil displacements obtained in the settlement analysis and construct the grid beam-spring model.

(3) Compute the sensitivities of foundation settlement with respect to adaptive reduced step-length of each pile and evaluate the optimal pile shortening by using the simplex method (Vanderplaats 1984). The adaptive step-length is taken as several meters in the initial design process for the computational efficiency and 1(m) in the final convergent design stage for the reliability of convergence. In this computation, the raft spring stiffness and the pile spring stiffness in the last step are used for computational efficiency.

(4) Update the pile spring stiffness and conduct the FEM analysis with the hybrid model for obtaining the settlement (process (1) in the flowchart of Fig. 7).
(5) Repeat the above procedure until the settlement reaches the target value.

It is important to note that, in order to overcome the difficulty of local optimality, the effect of several step sizes has been investigated in detail. Furthermore it was made clear that initial values have to be changed appropriately.

4. Simulation analysis 1: Example for basic model

The proposed optimization technique explained in Section 3 is applied to two cases, one for a low-rise building and the other for a high-rise building.

Fig. 8 illustrates two example ground models for low-rise and high-rise buildings. Fig. 9 indicates the load distribution (unit: kN/m^2). The allowable soil bearing stress is 70 (kN/m^2) for the case of the low-rise building and 500 (kN/m^2) for the case of the high-rise building. The target foundation settlement is 20 (mm) for both cases. The pile is placed for each column. The optimization is conducted for four cases: the pile-by-pile optimization, the one-grouping case (all the pile lengths are the same), two-grouping case and the three-grouping case. Fig. 10 presents the pile grouping for the three-grouping case (see Fig. 11 for two-grouping case). The move limit is 1-5 (m).

Table 1 shows the comparison of total optimal pile length for different groupings (unit: m). Fig. 11 illustrates the corresponding optimal pile placement (upper: pile force (kN), lower: pile length (m)) (diameter of circle indicates pile length). Since unsymmetrical pile placement has been obtained in the case of the pile-by-pile optimization case, that placement is not shown in Fig. 11 from the viewpoint of practicality.

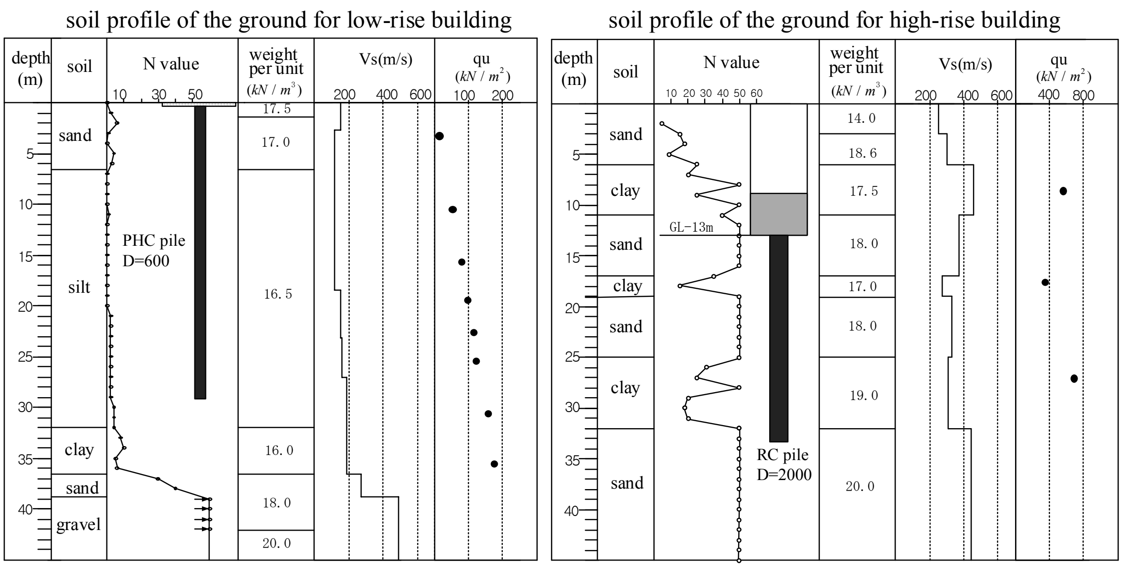

Fig. 8 Two example ground models

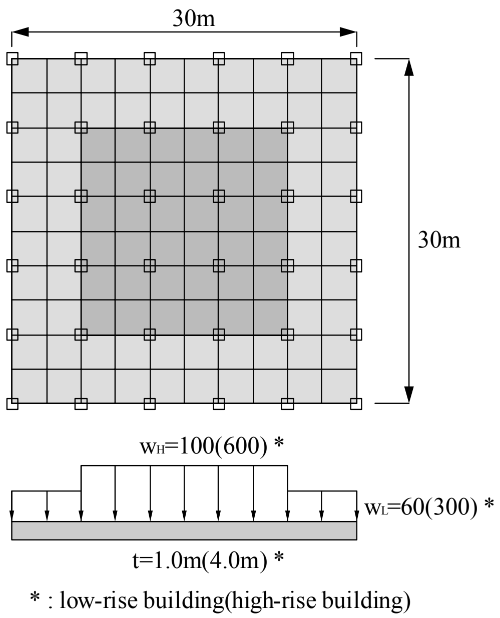

Fig. 9 Load distribution (unit: kN/m^2)

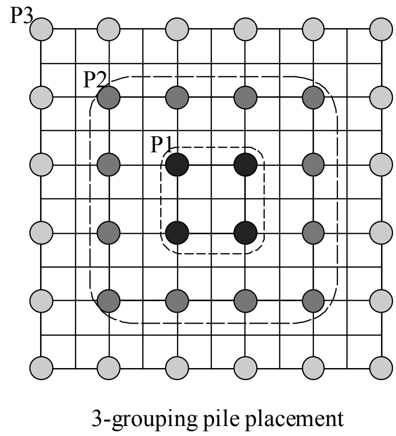

Fig. 10 Pile grouping (3-grouping)

Table 1 Comparison of total optimal pile length for different grouping (unit: m)

building	One grouping	2- grouping	3-grouping	Pile-by-pile
low-rise building	900	640	692	761
high-rise building	648	560	544	483

Fig. 12 indicates the settlement distribution at the middle cross-section, the pile force distribution, the contact stress distribution beneath the foundation and the bending moment distribution of the foundation beam for a low-rise building model. On the other hand, Fig. 13 presents those distributions for a high-rise building model. From these results (especially Table 1), it is found that the total pile length is the longest in the case of the one-grouping case and it is shorter in the case of the pile-by-pile optimization and the three-grouping case in a high-rise building. In a row-rise building, a little bit peculiar phenomenon occurs. As for the distribution of pile lengths, the outer ones, the inner ones and the intermediate ones are the order of lengths (the intermediate ones are longest) in the case of the low-rise building. On the other hand, the outer ones, the intermediate ones and the inner ones are the order of lengths (the inner ones are longest) in the case of the high-rise building.

In view of the comparison between the pile-by-pile optimization and the pile grouping, while a similar tendency is observed in the case of the low-rise building, a symmetrical property cannot be seen in the case of the pile-by-pile optimization. Based on this observation, it seems that the pile-by-pile optimization is hard to employ in the practical design. Furthermore, it is found that the intermediate piles are the longest in the case of the low-rise building and the inner piles are the longest in the case of the high-rise building.

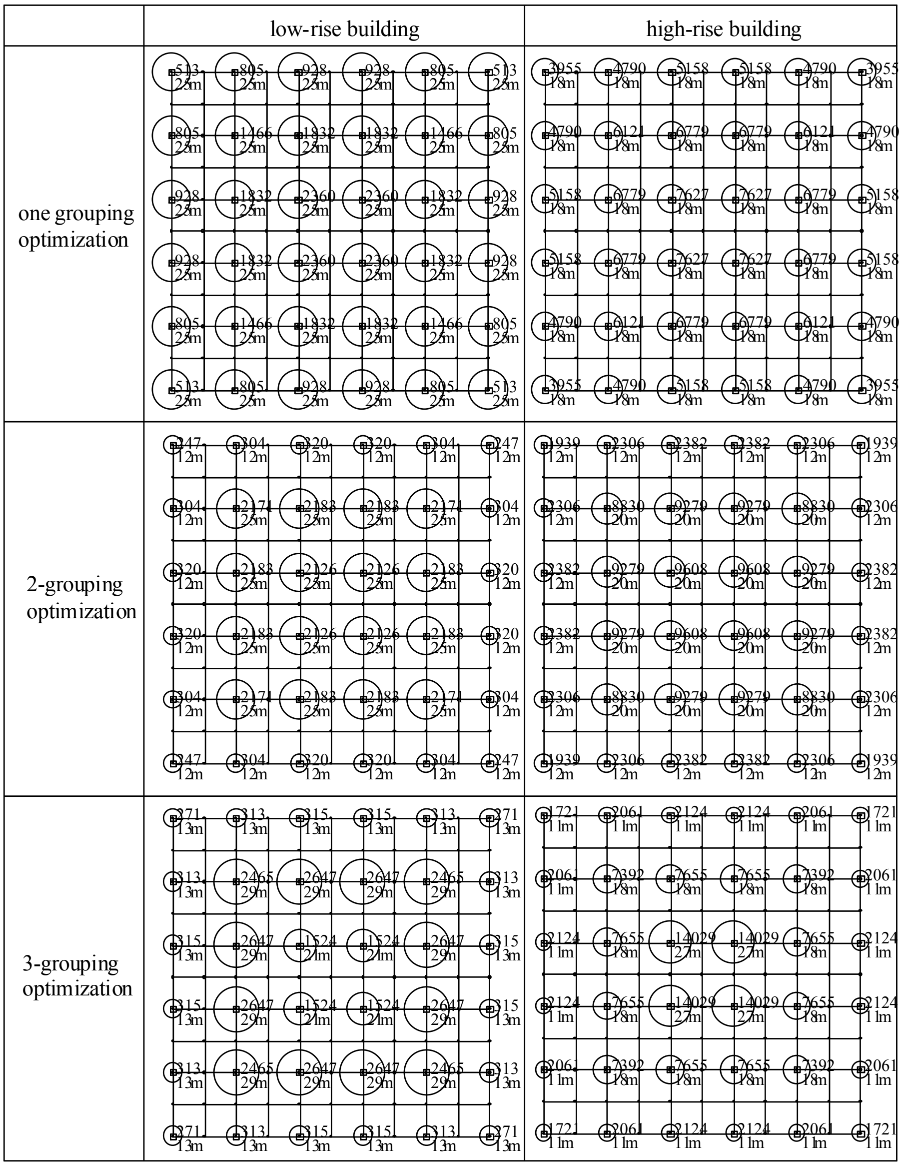

Fig. 11 Optimal pile placement (upper: pile force (kN), lower: pile length (m)) (diameter of circle indicates pile length)

In view of the settlement distribution, the difference of settlement between the outer part and the inner part is the largest in the case of the one-grouping and the bending moment in the foundation beam becomes larger. On the other hand, the difference of settlement between the outer part and the inner part becomes smaller in the case of the pile-by-pile optimization and the three-grouping and the bending moment in the foundation beam becomes smaller. It can be concluded that the cases of the pile-by-pile optimization and the three-grouping are rational in view of the relative settlement distribution and the bending moment distribution.

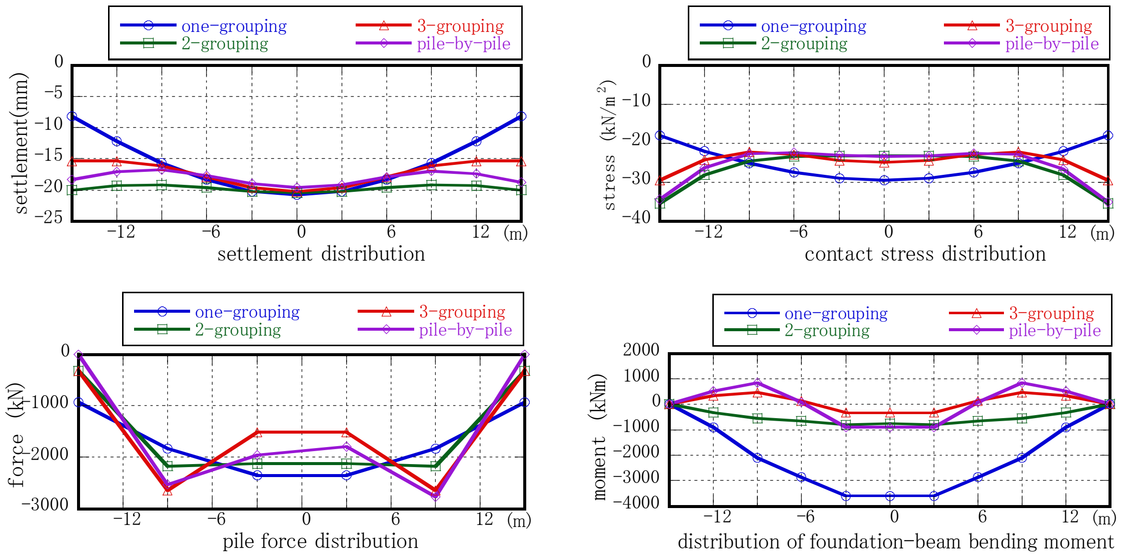

Fig. 12 Low-rise building model

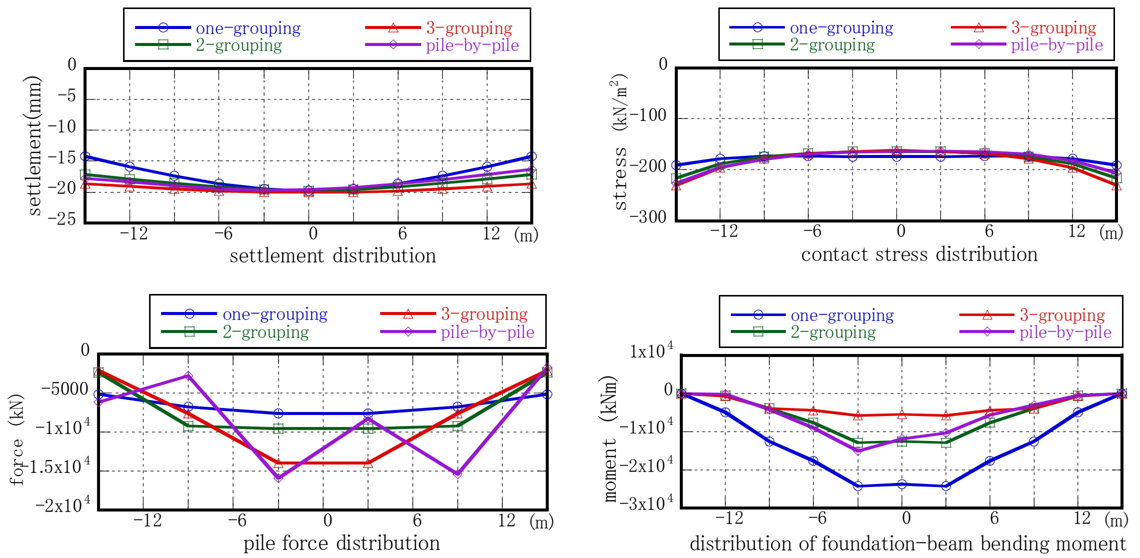

Fig. 13 High-rise building model

5. Simulation analysis 2

Piled raft foundations in actual buildings are treated here and measurements of foundation settlement during construction are investigated through the comparison with the optimized results. The accuracy of the proposed simplified analysis of foundation settlement is verified and the reliability of the proposed optimization technique is also discussed.

5.1 Low-rise building on soft ground

Consider a three-story reinforced concrete building with a piled raft foundation on a soft ground.

Fig. 14 shows the building plan and measurement points of pile force and settlement. The soil profile is the same as that for a low-rise building in Fig. 8. The thickness of the foundation slab is 600 (mm), the thickness of the outer wall is 180 (mm) and the piles are the PHC buried piles of the diameter 600 (mm) and the length 26 (m). The average load is 74 (kN/m^2). Fig. 15 illustrates an analysis model and load distribution. The foundation slab and walls are modeled by equivalent beams and the loads are applied at the nodes.

5.1.1 Comparison of simplified settlement analysis and actual measurement

Fig. 16 indicates the analysis result and measured result of settlement (unit: mm) and Fig. 17 presents the analysis result and measured result of contact pressure and pile force. It can be observed that the analysis result 17 (mm) of foundation settlement corresponds well with the measured result 16 (mm). The analysis result of the contact pressure beneath the foundation also

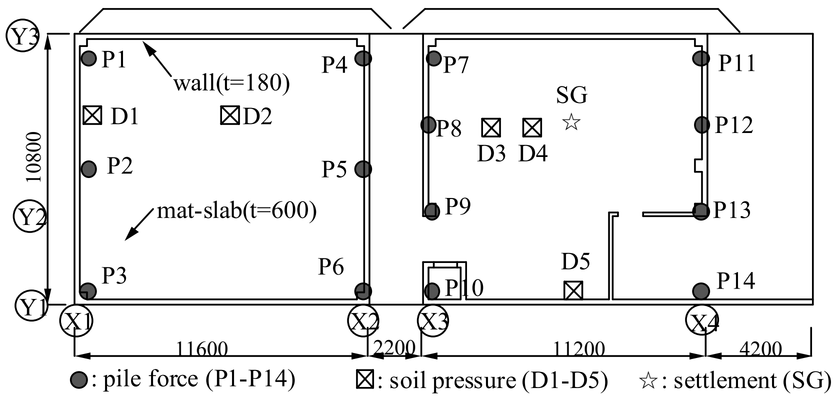

Fig. 14 Building plan and measurement points of pile force and settlement

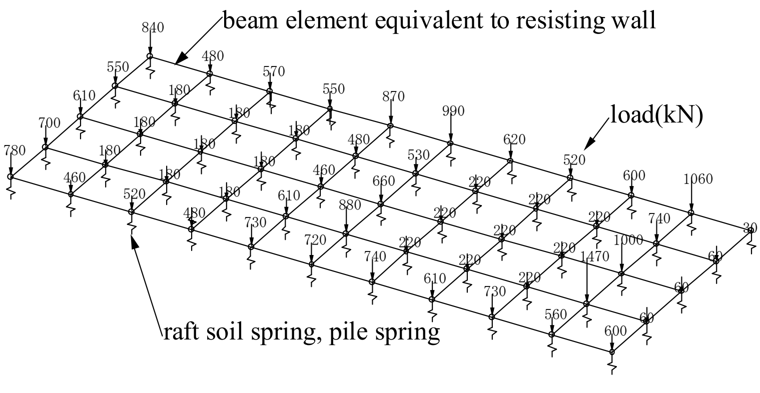

Fig. 15 Analysis model and load distribution

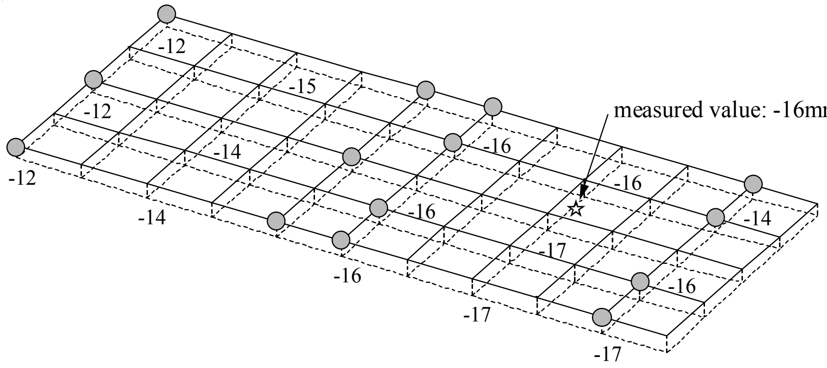

Fig. 16 Analysis result and measured result of settlement (unit: mm)

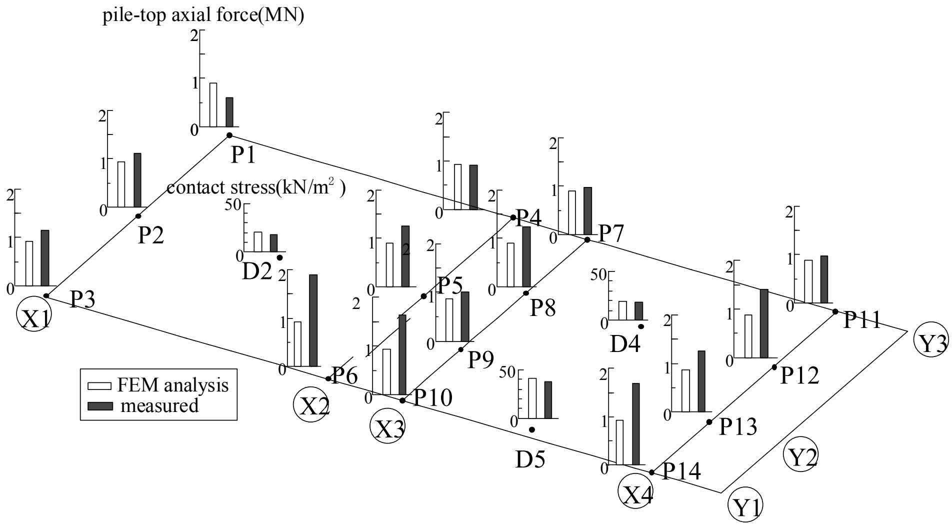

Fig. 17 Analysis result and measured result of contact pressure and pile force

corresponds well with the measured result. As for the pile force, although the measured value in the Y1 line is a little bit larger than the corresponding analysis result, most of the pile forces correspond well. The consolidation settlement is not considered because the preconsolidation stress of silty strata is larger than the overburden pressure. In addition, the buoyancy pressure is not taken into account in the FEM analysis because the water level is below the foundation bottom line.

5.1.2 Example of optimal pile placement

In the optimal pile placement, the target settlement is set to 15 (mm) in order to enable the comparison with the actual building and the initial value of the pile length (pile diameter is 600 (mm)) is given as 40 (m). The optimization has been conducted as follows: (1) pile-by-pile optimization with piles at all the nodes, (2) placing piles at corners and central nodes of resisting walls and introducing grouping optimization with the same grouping for X1-X2 lines and X3-X4 lines, (3) using the same pile placement as the actual one and employing the same grouping as that in (2).

Fig. 18 shows the comparison of optimal pile placements (Actual pile placement and length, actual pile placement and optimal length, pile-by-pile optimization, optimization by pile grouping). Although the total pile length is the shortest in the pile-by-pile optimization, the result seems to be irregular and unrealistic. In the second optimization, the total pile length becomes larger than the actual one. In the third optimization, although the pile lengths are different in two areas, the total pile length is almost the same as the actual one. This means that the actual placement is almost the optimal one.

Fig. 19 illustrates the settlement distributions (unit: mm) for these three optimization cases and the actual one.

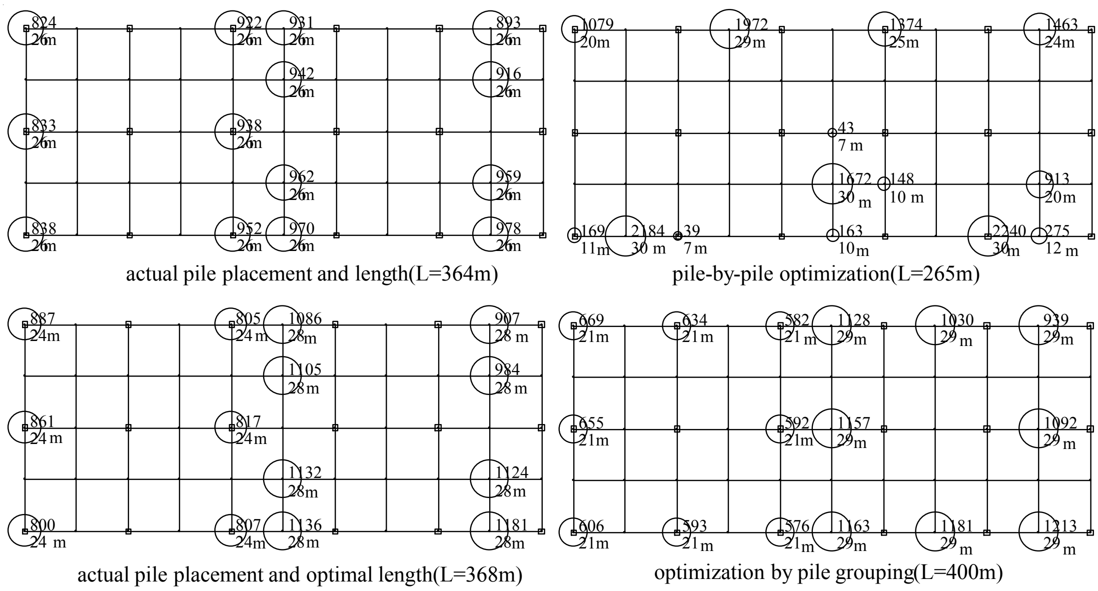

Fig. 18 Comparison of optimal pile placements

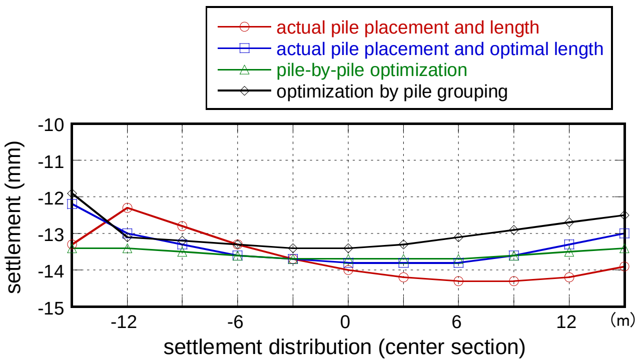

Fig. 19 Settlement distribution (unit: mm)

5.2 High-rise building supported by intermediate hard soil

The buildings consist of a high-rise building (19-story steel building) and a low-rise building (3-story reinforced concrete building). Consider first a high-rise building supported by intermediate hard soil. In this case, the silt soil exists beneath the intermediate sand soil. If the mat-slab or footing is used in this case, the settlement becomes large and the boundary stress between the high-rise building and the low-rise building becomes large. This leads to the installation of a piled raft foundation beneath the high-rise building.

Fig. 20 indicates the building cross-section and soil profile and Fig. 21 shows the building plan, pile location and measurement points. Consider next both the high-rise building and the low-rise building. The average loading at the high-rise building is 183 (kN/m^2) and that at the low-rise building is 96 (kN/m^2). The overall average is 134 (kN/m^2). The sand soil at GL-(5-12) (m) has the SPT count of 20 and GL-(12-21) (m) has the combination of clay and sand. The silt soil of the SPT count of 5 exists until GL-39 (m) and the gravel of the SPT count larger than 50 exists in deeper soil. The pile has a diameter of 800 (mm) in most parts and 1000 (mm) around the node. All the pile lengths are 10 (m) and 1 through 5 piles are placed depending on the loading. The water level is GL-2 (m).

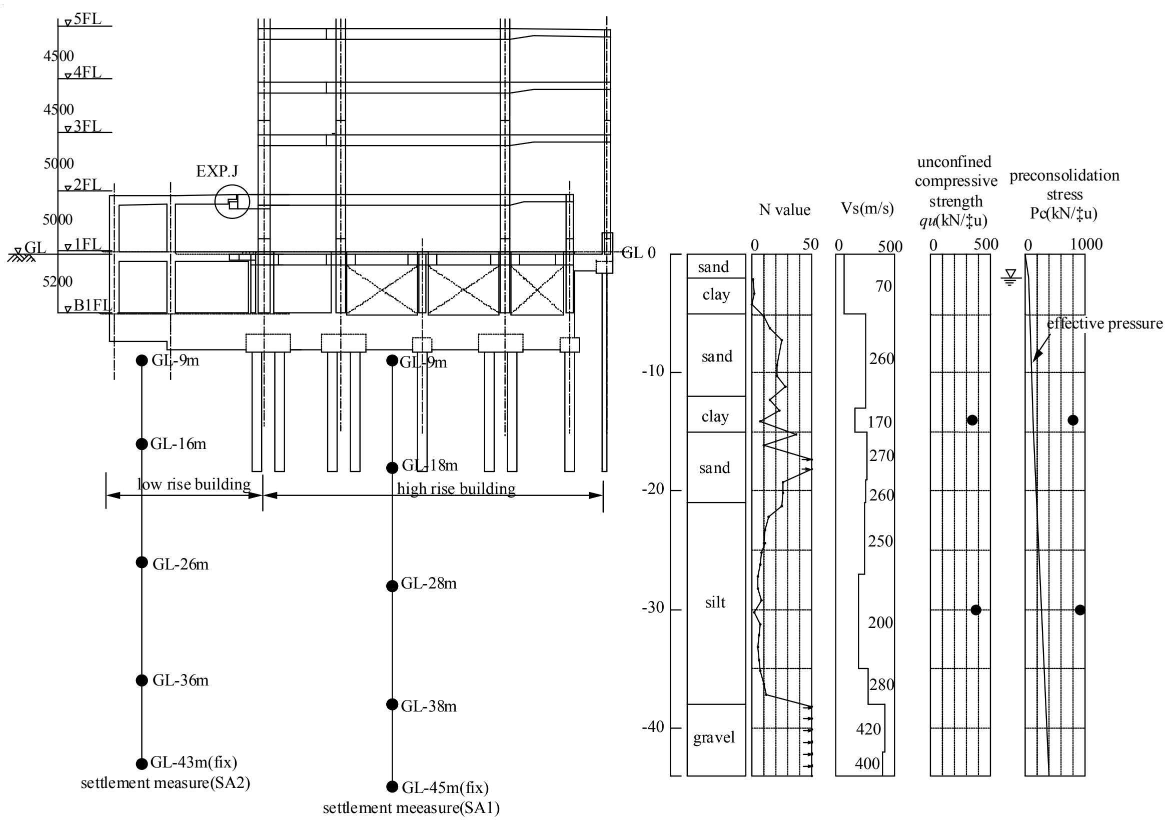

Fig. 20 Building cross-section and soil profile

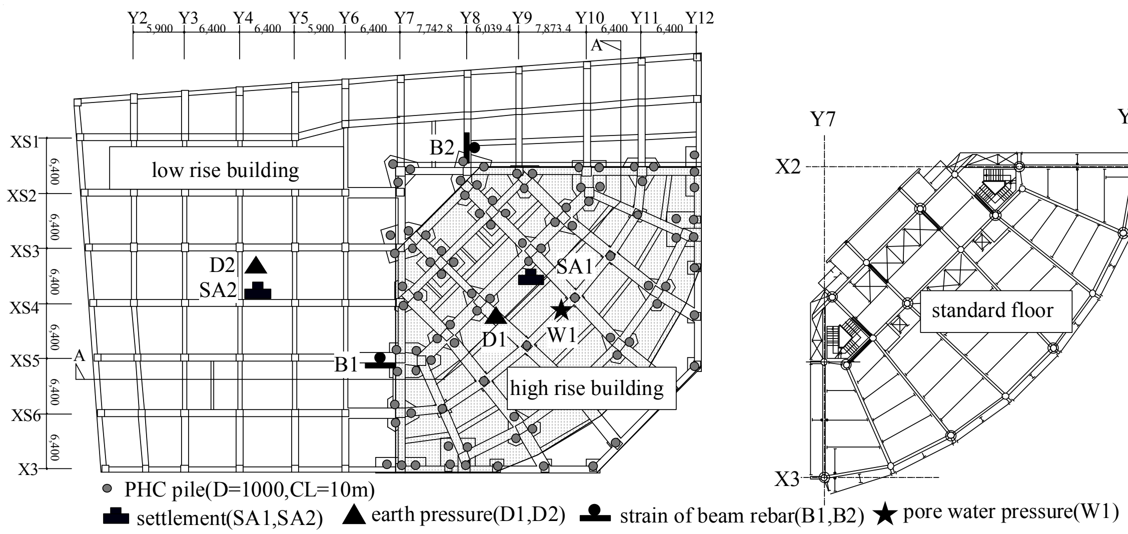

Fig. 21 Building plan, pile location and measurement points

5.2.1 Comparison of simplified settlement analysis and actual measurement

Fig. 22 illustrates the FEM analysis model and loads (kN). The buoyancy is considered in order to enable the comparison with the measured results. The soil Young's modulus is set differently beneath the low-rise building and the high-rise building in order to take into account the difference of average loading values. The consolidation settlement is not considered because the preconsolidation stress of clay strata is larger than the overburden pressure.

Fig. 23 presents the analysis result and measured value of settlement (unit: mm). The analysis value 17.8 (mm) at the center beneath the high-rise building corresponds well with the measured value 17 (mm). On the other hand, the analysis value 7.2 (mm) at the center beneath the low-rise building corresponds well with the measured value 10 (mm).

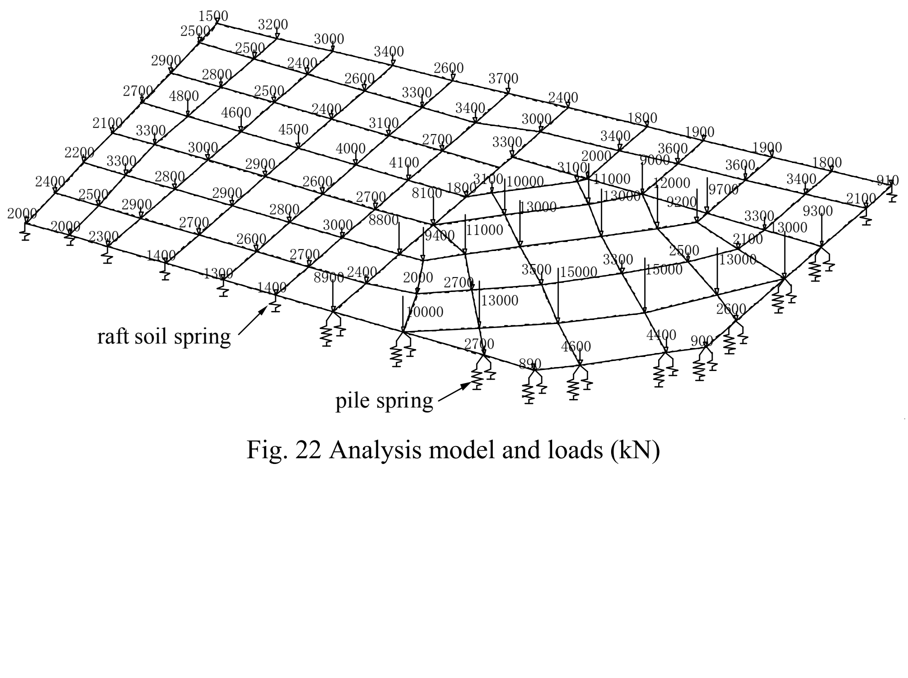

Fig. 22 Analysis model and loads (kN)

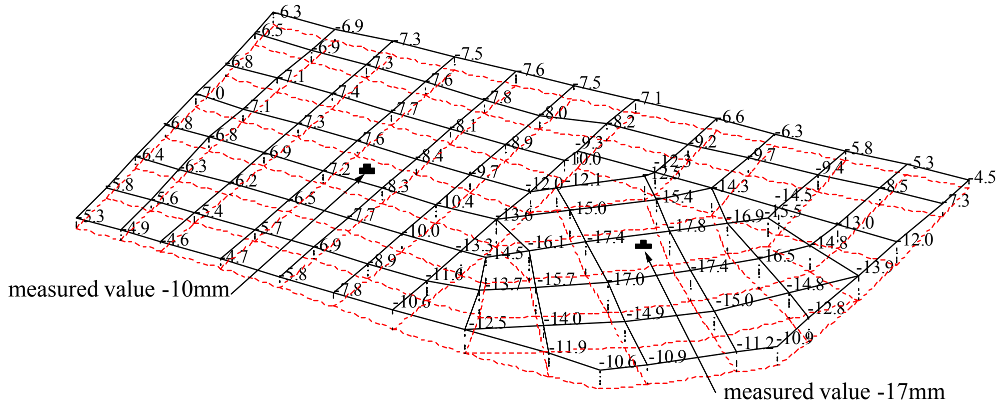

Fig. 23 Analysis result and measured value of settlement (unit: mm)

In Fig. 23, the stiffness reduction of soil due to the decrease of the confined pressure during construction (excavation) is considered. When the excavation is conducted, the decrease of the Young's moduli after excavation can be evaluated by the following equation due to Tamaoki *et al.* (1993a, b).

$$\frac{E_0'}{E_0} = \left(\frac{\sigma_{v0} - \Delta\sigma_v}{\sigma_{v0}} \right)^{0.4} \tag{16}$$

where E_0, E_0' (kN/m^2) are the Young's moduli before and after excavation, σ_{v0} (kN/m^2) is the effective stress before excavation and $\Delta\sigma_v$ (kN/m^2) is the decrease in the effective stress. This decrease in the effective stress can be evaluated by the equation due to Steinbrenner and Newmark (Steinbrenner 1934, 1936, Newmark 1935, Ohsaki 1991, Hirai 2013).

$$\Delta\sigma_v = \frac{2w}{\pi} \left\{ \frac{ab}{\sqrt{a^2+b^2+1}} \frac{a^2+b^2+2}{(a^2+1)(b^2+1)} + \sin^{-1} \frac{ab}{\sqrt{(a^2+1)(b^2+1)}} \right\} \tag{17}$$

where $a = (B/2)/Z_i$, $b = (L/2)/Z_i$, w (kN/m^2) is the excavation load, B, L (m) are the foundation width and length and Z_i (m) is the distance from the center of the i-th layer to the excavation plane.

5.2.2 Example of optimal pile placement

Consider another actual building. In this building, the same pile diameter and the same pile length are used and the number of piles at one place is varied depending on the loading value. The buoyancy is not considered and the target settlement value is 30 (mm). The group pile effect is considered when multiple piles are employed. The initial values are the pile diameter 800 (mm), the pile length 10 (m) and the number 6 of piles at one place. Three optimizations are used: (1) pile-by-pile optimization, (2) the same pile grouping as the actual one and (3) the pile grouping for 45-degree direction following the actual design. Fig. 24 indicates the optimal placement for high-rise building (upper: pile force (kN), lower: number of piles) and Fig. 25 shows the comparison of settlements by different optimizations (A-A cross-section in Fig. 21). The total pile length is the shortest in the case of the optimization (1) (pile-by-pile). However it seems that the pile grouping is preferable from the viewpoint of practicality (symmetricity of pile placement). As for the settlement distribution, the foundation settlement becomes large in the case of pile-by-pile optimization due to the small number of piles. However most of the distributions correspond fairly well.

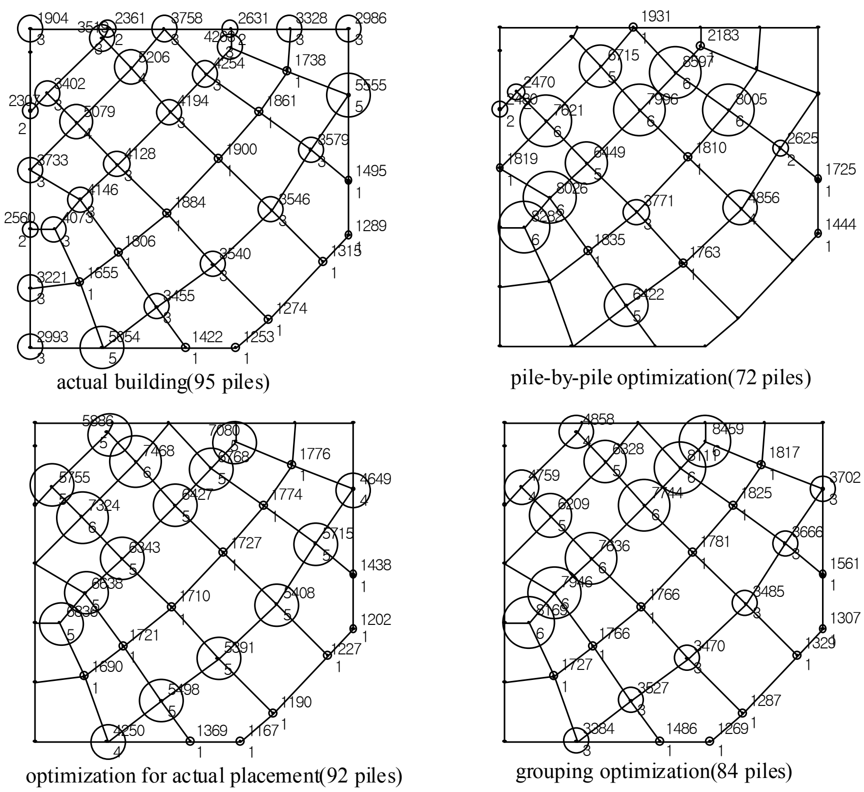

Fig. 24 Optimal placement for high-rise building (upper: pile force (kN), lower: number of piles)

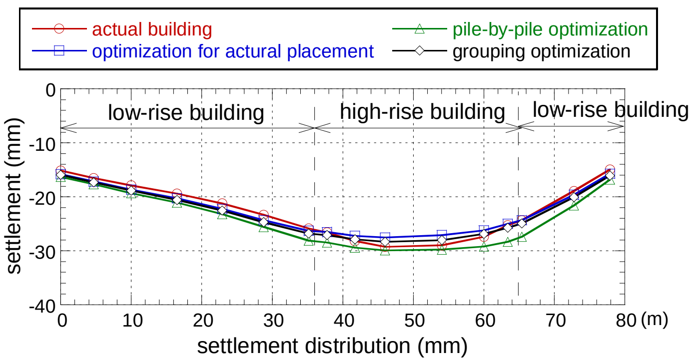

Fig. 25 Comparison of settlements by different optimizations (A-A cross-section in Fig. 21)

6. Conclusions

The following conclusions have been obtained.

(1) A simplified settlement analysis method for piled raft foundations has been proposed. The method takes into account the raft-pile-soil interaction concisely within an acceptable accuracy and uses Steinbrenner's equation.

(2) An optimal design problem has been formulated for determining pile lengths of piled raft foundations. The total pile length has been minimized under the settlement constraint on the foundation. An extended sequential linear programming technique combined with an adaptive step-length algorithm of pile lengths has been devised to solve the optimal design problem. It has been shown that the pile grouping is effective for obtaining practically acceptable pile placements. In order to overcome the difficulty of local optimality, initial values have to be changed appropriately. This kind of systematic algorithms for optimization of piled raft foundations is a first attempt and has a potential to further reliable development.

(3) The accuracy of the proposed simplified settlement analysis method and the validity of the obtained optimal solution have been investigated through the comparison with the actual measurement results in existing piled raft foundations.

References

Architectural Institute of Japan (AIJ) (2001a), Recommendations for Design of Building Foundations, Section 7.3, Piled raft foundation, 339-348.

Architectural Institute of Japan (AIJ) (2001b), Recommendations for Design of Building Foundations, Section 6.3, Vertical bearing strength and settlement, 200-237.

Chan, C.M., Zhang, L.M. and Ng, J.T.M. (2009), "Optimization of pile groups using hybrid genetic algorithms", *J. Geotech. Geoenviron. Eng., ASCE*, **135**(4), 497-505.

Chow, Y.K., Yong, K.Y. and Shen, W.Y. (2001), "Analysis of piled raft foundations using a variational approach", *Int. J. Geomechanics*, **1**(2), 129-147.

Cunha, R.P., Poulos, H.G. and Small, J.C. (2001), "Investigation of design alternatives for a piled raft case history", *J. Geotech. Geoenviron. Eng., ASCE*, **127**(8), 635-641.

Fattah, M.Y., Al-Mosawi, M.J. and Al-Zayadi, A.O. (2013), "Time dependent behavior of piled raft foundation in clayey soil", *Geomech. Eng., Int. J.*, **5**(1), 17-36.

Hardin, B.O. and Drnevich, V.P. (1972), "Shear modulus and damping in soils: Design equations and curves", *J. Soil Mech. Found. Div.*, **98**(SM7), 667-692.

Hirai, H. (2013), "Settlements and stresses of multi-layered grounds and improved grounds by equivalent elastic method", *Int. J. Numer. Anal. Meth. Geomech.*, **32**(5), 523-557.

Horikoshi, K. and Randolph, M.F. (1998), "A contribution to optimum design of piled rafts", *Geotechnique*, **48**(3), 301-317.

Kim, K.N., Lee, S.-H., Kim, K.-S., Chung, C.-K., Kim, M.M. and Lee, H.S. (2001), "Optimal pile arrangement for minimizing differential settlements in piled raft foundations", *Comput. Geotech.*, **28**(4), 235-253.

Kim, H.T., Yoo, H.K. and Kang, I.K. (2002), "Genetic algorithm-based optimum design of piled raft foundations with model tests", *Geotech. Eng.*, **33**(1), 1-11.

Leung, Y.F. (2010), "Foundation optimisation and its application to pile reuse", Ph.D. Thesis, Cambridge University, UK.

Leung, Y.F., Klar, A. and Soga, K. (2010), "Theoretical study on pile length optimization of pile groups and piled rafts", *J. Geotech. Geoenviron. Eng., ASCE*, **136**(2), 319-330.

Liew, S.S., Gue, S.S. and Tan, Y.C. (2002), “Design and instrumentation results of a reinforcement concrete piled raft supporting 2500 ton oil storage tank on very soft alluvium deposits”, *Proceedings of 9th International Conference on Piling and Deep Foundations*, Deep Foundations Institute, 263-269.

Newmark, N.M. (1935), *Simplified Computation of Vertical Pressures in Elastic Foundation*, Circular No. 24, Engineering Experiment Station, University of Illinois.

Ohsaki, Y. (1991), *Building Foundation Engineering*, Gihodo Press, Tokyo.

Poulos, H.G., Small, J.C., Ta, L.D., Sinha, J. and Chen, L. (1997), “Comparison of some methods for analysis of piled rafts”, *Proceedings of 14th Conference on Soil Mechanics and Foundation Engineering*, **2**, Balkema, Rotterdam, The Netherlands, 1119-1124.

Poulos, H.G. (2001), “Piled raft foundations – Design and applications”, *Geotechnique*, **51**(2), 95-113.

Prakoso, W.A. and Kulhawy, F.H. (2001), “Contribution to piled raft foundation design”, *J. Geotech. Geoenviron. Eng., ASCE*, **127**(1), 17-24.

Randolph, M.F. (1983), Design of piled raft foundations, *CUED/D TR 143*, Cambridge University, UK.

Randolph, M.F. (1994), Design methods for pile groups and piled rafts, *XIII CIMSTF*, New Delhi.inde, 61-82.

Reul, O. and Randolph, M.F. (2003), “Piled rafts in overconsolidated clay: comparison of in situ measurements and numerical analyses”, *Geotechnique*, **53**(3), 301-315.

Reul, O. and Randolph, M.F. (2004), “Design strategies for piled rafts subjected to nonuniform vertical loading”, *J. Geotech. Geoenviron. Eng., ASCE*, **130**(1), 1-13.

Small, J.C. and Zhang, H.H. (2002), “Behavior of piled raft foundations under lateral and vertical loading”, *Int. J. Geomech.*, **2**(1), 29-45.

Steinbrenner, W. (1934), Tafeln zur Setzungsberechnung, *Die Straße*, Vol. 1.

Steinbrenner, W. (1936), *Bodenmechanik und neizeitlicher Straßenbau*, (Symposium by 24 authors), Volk und Reich Verlag, Berlin, Germany.

Ta, L.D. and Small, J.C. (1996), “Analysis of piled raft systems in layered soils”, *Int. J. Numer. Anal. Method. Geomech.*, **20**(1), 57-72.

Tamaoki, K., Katsura, Y., Nishio, S. and Kishida, S. (1993a), “Estimation of Young’s moduli of bearing soil strata”, *Excavation in Urban Areas*, *KIG Forum’93*, (*T. Adachi Edition*), *Jap. Soc. Soil Mech. Found. Eng.*, 23-33.

Tamaoki, K., Katsura, Y. and Kishida, S. (1993b), “Young’s moduli of bearing strata estimated from vertical deformation during excavation and construction”, *J. Struct. Constr. Eng., AIJ*, No. 446, 73-80. [In Japanese]

Valliappan, S., Tandjiria, V. and Khalili, N. (1999), “Design of raft-pile foundation using combined optimization and finite element approach”, *Int. J. Numer. Anal. Meth. Geomech.*, **23**(10), 1043-1065.

Vanderplaats, G.N. (1984), *Numerical Optimization Techniques for Engineering Design with Applications*, McGraw-Hill.

CC

Appendix 1. The settlement coefficient $I_S(H_k, v_{Sk})$

The settlement coefficient $I_S(H_k, v_{Sk})$ in Eq. (3) is expressed by

$$I_S(H_k, v_{Sk}) = (1 - v_{Sk}^2)F_1(H_k) + (1 - v_{Sk} - 2v_{Sk}^2)F_2(H_k) \tag{A1}$$

$$F_1(H_k) = \frac{1}{\pi}\left\{ l \cdot \log_e \frac{\left(1+\sqrt{l^2+1}\right)\sqrt{l^2+d_k^2}}{l\left(1+\sqrt{l^2+d_k^2+1}\right)} + \log_e \frac{\left(1+\sqrt{l^2+1}\right)\sqrt{1+d_k^2}}{l+\sqrt{l^2+d_k^2+1}} \right\} \tag{A2}$$

$$F_2(H_k) = \frac{d_k}{2\pi}\tan^{-1}\frac{l}{d_k\sqrt{l^2+d_k^2+1}} \tag{A3}$$

where $l = (L/2)/(B/2)$, $d_k = H_k/(B/2)$.